JACC: CARDIOVASCULAR INTERVENTIONS VOL. ■, NO. ■, 2019

PUBLISHED BY ELSEVIER

Myocardial Blood Flow and Coronary Flow Reserve During 3 Years Following Bioresorbable Vascular Scaffold Versus Metallic Drug-Eluting Stent Implantation

The VANISH Trial

Wijnand J. Stuijfzand, MD,[a,*] Stefan P. Schumacher, MD,[a,*] Roel S. Driessen, MD,[a] Adriaan A. Lammertsma, PhD,[b] Amber L. Bakker, BSc,[a] Mischa T. Rijnierse, MD, PhD,[a] Albert C. van Rossum, MD, PhD,[a] Peter M. van de Ven, PhD,[c] Alexander Nap, MD, PhD,[a] Yolande Appelman, MD, PhD,[a] Niels van Royen, MD, PhD,[d] Maarten A. van Leeuwen, MD,[e] Jorrit S. Lemkes, MD,[a] Pieter G. Raijmakers, MD, PhD,[b] Paul Knaapen, MD, PhD[a]

ABSTRACT

OBJECTIVES The randomized clinical VANISH (Impact of Vascular Reparative Therapy on Vasomotor Function and Myocardial Perfusion: A Randomized [^{15}O]H_2O PET/CT Study) trial was conducted to assess quantitative myocardial blood flow (MBF) during resting, hyperemia, and cold pressor testing (CPT) with positron emission tomographic perfusion imaging after the implantation of a bioresorbable everolimus-eluting scaffold compared with a drug-eluting stent.

BACKGROUND Long-term resorption of the bioresorbable everolimus-eluting scaffold reinstates normal vessel geometry, allowing natural regeneration of the newly formed endothelium with revival of vasomotor function.

METHODS Sixty patients (18 to 65 years of age) with single-vessel disease and type A or B1 lesions were randomized in a 1-to-1 fashion. Approximately 1 month, 1 year, and 3 years after device implantation, patients underwent [^{15}O]H_2O cardiac positron emission tomography. The primary endpoint was the interaction of device type and evolution over time of hyperemic MBF, coronary flow reserve, or CPT reserve. At 3-year follow-up, control invasive coronary angiography with optical coherence tomography was performed.

RESULTS Fifty-nine (98%), 56 (93%), and 51 (85%) patients successfully completed 1-month, 1-year, and 3-year follow-up positron emission tomography, respectively, and no culprit vessel events were registered during follow-up time. The primary study endpoint (i.e., interaction between device type and time) was nonsignificant for hyperemic MBF, CPT reserve, and coronary flow reserve ($p > 0.05$ for all). In all patients, hyperemic MBF decreased from 1 to 3 years ($p = 0.02$), while coronary flow reserve was lower at 3-year follow-up compared with 1-month and 1-year follow-up ($p = 0.03$ for both). After 3 years, percentage area stenosis measured with optical coherence tomography was higher within the bioresorbable everolimus-eluting scaffold compared with the drug-eluting stent ($p = 0.03$).

CONCLUSIONS The hypothesized beneficial effects of scaffold resorption did not translate to improved MBF during maximal hyperemia or endothelium-dependent vasodilation by CPT. (J Am Coll Cardiol Intv 2019;■:■-■) © 2019 by the American College of Cardiology Foundation.

From the [a]Department of Cardiology, Amsterdam UMC, Location VU University Medical Center, Amsterdam, the Netherlands; [b]Department of Radiology and Nuclear Medicine, Amsterdam UMC, Location VU University Medical Center, Amsterdam, the Netherlands; [c]Department of Epidemiology and Biostatistics, Amsterdam UMC, Location VU University Medical Center, Amsterdam, the Netherlands; [d]Department of Cardiology, Radboud University Medical Center, Nijmegen, the Netherlands; and the [e]Department of Cardiology, Isala Heart Center, Zwolle, the Netherlands. *Drs. Stuijfzand and Schumacher contributed equally to this work. This study was sponsored in part by Abbott Vascular and the Dutch Heart Foundation (grant 2013T078). The authors have reported that they have no relationships relevant to the contents of this paper to disclose.

Manuscript received December 3, 2018; revised manuscript received February 4, 2019, accepted March 5, 2019.

ISSN 1936-8798/$36.00 https://doi.org/10.1016/j.jcin.2019.03.004

ABBREVIATIONS AND ACRONYMS

%AS = percentage area stenosis

%DS = percentage diameter stenosis

BVS = bioresorbable everolimus-eluting scaffold

CAD = coronary artery disease

CFR = coronary flow reserve

CPT = cold pressor test

DES = drug-eluting stent

ICA = invasive coronary angiography

MBF = myocardial blood flow

MLA = minimal luminal area

MLD = minimal luminal diameter

OCT = optical coherence tomography

PCI = percutaneous coronary intervention

PET = positron emission tomographic

QCA = quantitative coronary angiography

RPP = rate-pressure product

The completely bioresorbable everolimus-eluting scaffold (BVS) has been developed to improve long-term outcomes of percutaneous coronary intervention (PCI). The long-term resorption of the BVS restores normal vessel geometry, allowing natural regeneration of the endothelium because of preferential shear stress, blood flow, and cyclic strain patterns (1-3). Moreover, favorable epicardial blood flow and flow-mediated coronary dilatation after BVS resorption could significantly aid in restoration of vasoactivity and long-term myocardial perfusion, which is among the most important independent prognostic predictors of adverse events and death in ischemic heart disease (4,5). After resorption of the BVS, the treated coronary artery may regain its responsiveness to sympathetic stimuli, inducing endothelial-dependent vasodilation. Cold pressor testing is considered the gold standard for the evaluation of sympathetic function, and an impaired response to a cold pressor test (CPT) is associated with the risk for developing cardiovascular events (6). Data to substantiate these postulated effects after BVS implantation are, however, lacking. Therefore, a randomized clinical trial of the BVS versus a metallic drug-eluting stent (DES) was performed, using positron emission tomographic (PET) perfusion imaging to assess (hyperemic) myocardial blood flow (MBF), MBF during a CPT, and coronary flow reserve (CFR) over a 3-year period (VANISH [Impact of Vascular Reparative Therapy on Vasomotor Function and Myocardial Perfusion: A Randomized $[^{15}O]H_2O$ PET/CT Study]; NCT01876589).

METHODS

STUDY DESIGN AND PARTICIPANTS. The study design of the VANISH trial has been described in detail previously (7). The VANISH trial is a prospective, single-blind, randomized, 2-group, single-center clinical trial. Patients with de novo single-vessel coronary artery disease (CAD) (type A or B1 lesions) resulting in myocardial ischemia without biochemical signs of myocardial infarction and with normal left ventricular function (≥50%) were eligible for inclusion. Exclusion criteria were age >65 years, prior cardiac history, poor kidney function (estimated glomerular filtration rate <30 ml · min^{-1}), asthma, other than sinus rhythm, or pregnancy. After inclusion, randomization between implantation of the BVS or the metallic DES using the Absorb or XIENCE Prime (Abbott Vascular, Santa Clara, California) was performed in a 1-to-1 fashion. Patients were blinded to the implanted study device during the complete study follow-up. Study investigators and operators were instructed not to disclose treatment assignment to patients and referring physicians. Follow-up visits were planned approximately 1 month, 1 year, and 3 years after PCI. At every time point, $[^{15}O]H_2O$ PET was performed to assess resting MBF, CPT MBF, hyperemic MBF, CPT reserve, and CFR. Additionally, repeat invasive coronary angiography (ICA) with optical coherence tomography (OCT) of the treated coronary segment was included in the study protocol at 3-year follow-up. The primary endpoint of the study was the difference in the evolution of MBF during hyperemia, CFR, and CPT reserve over time between the 2 treatment arms. Written informed consent was obtained from all patients, and the ethics committee of the VU University Medical Center approved the study.

PCI AND OCT. ICA and PCI were performed on a monoplane cardiovascular x-ray system (Allura Xper FD 10/10, Philips Healthcare, Best, the Netherlands). Device dimensions were based on optical coherence tomographic measurements or quantitative coronary angiography (QCA). All device implantations were performed according to standard procedural guidelines. Lesion length had to allow for complete coverage of the lesion, including at least 2 mm of nondiseased tissue on either side of the target lesion. Post-dilatation was performed with a balloon shorter than the implanted device and was left to the discretion of the operator. Intravascular OCT was performed before and immediately after device implantation with automated injection of 3 or 4 ml · sec^{-1} contrast agent and automated pull-back set at 20 mm · sec^{-1}. All patients received at least 80 mg of aspirin daily for the study duration and 75 mg of clopidogrel daily for a minimum of 12 months after device implantation. Control ICA, including OCT of the originally stented segment, was performed at 3-year follow-up.

QUANTITATIVE CORONARY ANGIOGRAPHIC ANALYSIS. In all patients, quantitative coronary angiographic analyses were performed off-line by an analyst blinded to all other test results, with an automated contour analysis system (CAAS II, Pie Medical, Maastricht, the Netherlands). The small radiopaque markers at each end of the Absorb scaffold aided for localization of the nonradiopaque scaffold. Lesion length, reference vessel diameter, in-device minimal luminal diameter (MLD), and percentage diameter stenosis (%DS), were calculated using automated

contour analysis with manual correction when required. In-device binary restenosis at 3-year follow-up was defined as a ≥50% diameter stenosis.

OCT. Baseline and 3-year follow-up in-device cross sections were analyzed with a 1-mm interval by an analyst blinded to all other test results using patented offline software (ILUMIEN OPTIS, LightLab Imaging/St. Jude Medical, St. Paul, Minnesota). Luminal areas and diameters were calculated using semiautomated luminal contour detection and manually adjusted if necessary. Strut areas in both BVS and DES lying within the luminal contour were included in the luminal dimensions in case of good apposition or malapposition. Reference luminal area was defined as the average of the proximal and distal reference area, both selected as the frame with the largest luminal area within 5 mm of the device (8). Percentage area stenosis (%AS) was the ratio between minimal luminal area (MLA) and reference luminal area. Post-PCI scaffold and stent areas were measured at the endoluminal reflective edge of metallic struts, whereas in polymeric struts, the endoluminal bright border was used. At 3-year follow-up, the endoluminal edge of the black core of polymeric struts was considered as the endoluminal surface (9). The asymmetry index was calculated after PCI per lesion (1 – [lowest cross-sectional in-device minimum device diameter/highest cross-sectional maximum device diameter]). A lesion with an asymmetry index >0.3 was considered an asymmetrical lesion (10). The circularity of each in-device cross-section was evaluated after PCI through the eccentricity index: the minimum device diameter divided by the maximum device diameter. The cross section with the lowest eccentricity index was used for the analysis per lesion, with an eccentricity index <0.7 indicating an eccentric lesion (10). The scaffold/stent expansion index was calculated after PCI as the ratio of minimal endoluminal scaffold or stent area to the average reference luminal area. Optimal scaffold or stent expansion was present in case the expansion index was ≥90% or exceeded the luminal area of the reference segment with the lowest luminal area. If minimal endoluminal device area was ≥9 mm^2, optimal scaffold or stent expansion was defined as an expansion index of ≥80% (10). At 3-year follow-up, recognizable (former) polymeric struts with a black box and clear endoluminal and abluminal borders were used for analyses (11). Neointimal area was defined as the difference between endoluminal stent area and luminal area, corrected for extrastent lumen when present (9,12). Neointimal strut coverage was defined as the distance between the midpoint of the endoluminal strut surface and the luminal contour. Struts were classified as uncovered in case of strut coverage <30 and 0 μm for (former) polymeric and metallic struts, respectively. A strut was considered malapposed when the distance between the endoluminal strut surface and the luminal contour was more than the strut thickness (90 and 150 μm for metallic and [former] polymeric struts, respectively) (9).

PET IMAGING. PET studies using ^{15}O-labeled water were performed as described previously (13). The Ingenuity TF 128 PET/CT scanner (Philips Healthcare) was used for all PET studies. Patients were instructed to temporarily cease all vasoactive medication at least 5 pharmacological half-lives prior to the scan. First, scout computed tomographic study was performed for patient positioning, followed by a dynamic emission scan at rest, during the CPT, and during intravenous adenosine (140 $\mu g \cdot kg^{-1} \cdot min^{-1}$) induced hyperemia. The CPT was performed by immersing the left or right hand of the patient into melting ice water (0°C). A plastic tube, 30 × 15 cm, containing half ice cubes and half water, was used for the CPT. The tube was concealed by exploration of an expanded plastic glove within the ice water and on top of the open end of the plastic tube. The hand of the patient was introduced into the explored glove, which was surrounded by melting ice water, starting at least 90 seconds prior to the start of the scan, and was continued during the complete scan acquisition (14). Parametric MBF images were generated and analyzed quantitatively by an experienced analyst using Cardiac VUer (15). The analyst was blinded to all other study results. MBF was expressed in milliliters per minute per gram of perfusable tissue. MBF during rest, the CPT, and hyperemia was calculated for each of the 3 coronary territories, according to standard segmentation procedures (16). CFR was calculated as the ratio of hyperemic MBF to resting MBF, whereas CPT reserve was calculated as the ratio of CPT MBF to resting MBF. Target area was defined as the myocardial territory of a treated vessel, while remote myocardium was defined as the myocardial territory of the remaining nontreated vessels. To account for changes in resting MBF caused by cardiac work load, additional resting MBF values were obtained by correcting for rate-pressure product (RPP), an index of myocardial oxygen consumption, using the following equation: corrected MBF = (MBF/RPP) × 104. Subsequently, corrected CPT reserve and CFR values were calculated using resting corrected MBF.

STATISTICAL ANALYSES. Continuous variables are presented as mean ± SD, whereas categorical variables are expressed as actual numbers. Continuous

TABLE 1 Baseline Patient Characteristics (n = 60)

	BVS ± (n = 30)	DES ± (n = 30)	p Value
Age (yrs)	55 ± 7	55 ± 7	0.78
Male	23 (77)	22 (73)	0.77
Body mass index (kg · m^{-2})	26.7 ± 4.9	27.7 ± 4.5	0.43
CAD risk factors			
Hypertension	15 (50)	15 (50)	1.00
Hypercholesterolemia	8 (27)	8 (27)	1.00
Current smoking	18 (60)	11 (37)	0.12
History of smoking	3 (10)	9 (30)	0.10
Family history of CAD	17 (57)	17 (57)	1.00
Diabetes	2 (7)	4 (13)	0.67
Medication			
Antiplatelet therapy	28 (93)	29 (97)	1.00
ACE inhibitors	12 (40)	12 (40)	1.00
Beta-blockers	27 (90)	27 (90)	1.00
Statins	27 (90)	27 (90)	1.00
Dual antiplatelet agents	16 (53)	16 (53)	1.00
Long-acting nitrates	2 (7)	4 (13)	0.67
Indication			
Stable angina	18 (60)	24 (80)	0.16
Silent ischemia	–	1 (3)	NA
Unstable angina	12 (40)	5 (17)	0.08
Target artery			
LAD	16 (53)	20 (67)	0.43
RCA	6 (20)	8 (27)	0.76
Cx	8 (27)	2 (7)	0.08

Values are mean ± SD or n (%).

ACE = angiotensin-converting enzyme; BVS = bioresorbable everolimus-eluting scaffold; CAD = coronary artery disease; Cx = circumflex coronary artery; DES = drug-eluting stent; LAD = left anterior descending coronary artery; NA = not applicable; RCA = right coronary artery.

variables were analyzed using the independent-samples Student's *t*-test, or Mann-Whitney *U* test in case data were not normally distributed, unless otherwise stated. Categorical variables were analyzed using the Fisher exact test. A mixed-model analysis was used to analyze PET perfusion results using Bonferroni correction for multiple pairwise comparisons for localizing the source of the difference. On the basis of a total sample size of 25 per group, this study will have 80% power to detect differences in mean changes in outcomes between devices of at least 0.8 times the SD of the outcome. This calculation was based on a test for a nonzero difference in mean change score between 2 groups between 2 time points, assuming a within-subject correlation of 0.5 and 2-sided testing at a significance level of 5%. Statistical analyses were performed using SPSS version 20.0 (IBM, Armonk, New York).

RESULTS

From August 2013 to December 2014, 60 patients were enrolled and successfully randomized between the BVS and the DES. Table 1 lists the baseline characteristics of both treatment arms. Procedural and device implantation characteristics have been described previously (7). In the DES arm, 3 patients required additional device implantation because of significant

TABLE 2 Positron Emission Tomographic Perfusion Results

	1 Month	1 Year	3 Years	Interaction (DT × TP)	Main Effects	Delta 1 Month to 1 Year	Delta 1 Month to 3 Years
Resting MBF (ml · min^{-1} · g^{-1})							
BVS	1.02 ± 0.28	0.99 ± 0.24	1.05 ± 0.25		DT: p = 0.70; TP: p = 0.20	−0.05 ± 0.15	0.01 ± 0.22
DES	0.96 ± 0.24	1.00 ± 0.23	1.03 ± 0.26	p = 0.30		0.03 ± 0.22	0.06 ± 0.17
All	0.99 ± 0.26	0.99 ± 0.23	1.04 ± 0.26			−0.01 ± 0.19	0.03 ± 0.20
CPT							
BVS	1.20 ± 0.38	1.07 ± 0.30	1.17 ± 0.32		DT: p = 0.47; TP: p < 0.05	−0.12 ± 0.22	−0.02 ± 0.34
DES	1.08 ± 0.23	1.08 ± 0.25	1.15 ± 0.26	p = 0.14		0.00 ± 0.23	0.06 ± 0.20
All	1.14 ± 0.32	1.08 ± 0.27	1.16 ± 0.29*			−0.06 ± 0.23	0.02 ± 0.28
Hyperemic MBF (ml · min^{-1} · g^{-1})							
BVS	3.04 ± 0.80	3.20 ± 1.17	2.96 ± 0.92		DT: p = 0.46; TP: p < 0.05	0.16 ± 0.85	−0.03 ± 0.58
DES	3.33 ± 0.77	3.38 ± 0.83	3.02 ± 0.67	p = 0.21		0.05 ± 0.83	−0.41 ± 0.88
All	3.18 ± 0.79	3.29 ± 1.01	2.99 ± 0.80†			0.11 ± 0.83	−0.21 ± 0.76
CPT reserve							
BVS	1.16 ± 0.21	1.09 ± 0.14	1.13 ± 0.16		DT: p = 0.92; TP: p = 0.27	−0.05 ± 0.19	−0.02 ± 0.21
DES	1.15 ± 0.23	1.12 ± 0.20	1.14 ± 0.17	p = 0.86		−0.03 ± 0.26	−0.01 ± 0.25
All	1.16 ± 0.21	1.10 ± 0.17	1.13 ± 0.16			−0.04 ± 0.23	−0.01 ± 0.23
CFR							
BVS	3.09 ± 0.94	3.17 ± 0.99	2.87 ± 0.86		DT: p = 0.19; TP: p < 0.05	0.18 ± 0.99	−0.05 ± 0.94
DES	3.57 ± 0.85	3.45 ± 0.97	3.07 ± 0.84	p = 0.18		−0.10 ± 0.76	−0.57 ± 0.89
All	3.33 ± 0.92	3.31 ± 0.98	2.97 ± 0.85†‡			0.04 ± 0.89	−0.31 ± 0.95

Values are mean ± SD. Influence of DT and TP on absolute myocardial perfusion was calculated using a mixed-model analysis including two main effects (DT and TP) and a Bonferroni post hoc analysis when appropriate. Note that the delta values of the perfusion indexes display the change in patients who reached 1-year and 3-year follow-up. *p = 0.06 versus 1 year. †p = 0.02 versus 1 year. ‡p = 0.03 versus 1 month and 1 year.

CFR = coronary flow reserve; CPT = cold pressor test; DT = device type; MBF = myocardial blood flow; TP = time point; other abbreviations as in Table 1.

CENTRAL ILLUSTRATION **Interaction Between Device and Time for Hyperemic Myocardial Blood Flow, Coronary Flow Reserve, and Cold Pressor Test Reserve**

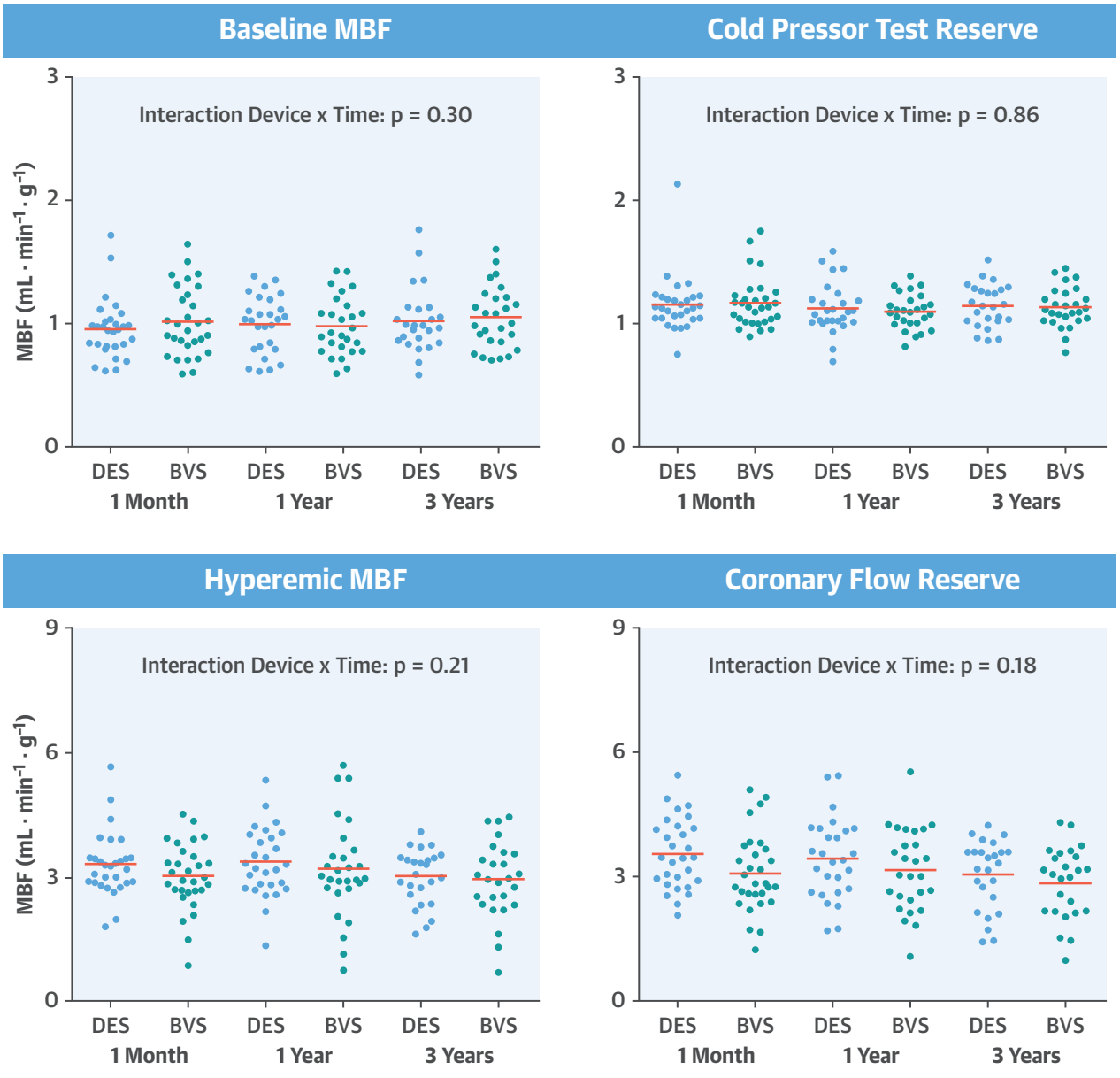

Stuijfzand, W.J. et al. J Am Coll Cardiol Intv. 2019;■(■):■-■.

Per patient absolute myocardial perfusion results are displayed, comparing bioresorbable everolimus-eluting scaffold (BVS) and drug-eluting stent (DES), measured with [^{15}O] H_2O positron emission tomography 1 month, 1 year, and 3 years after device implantation, respectively. The **red horizontal lines** represent the means. P values show the nonsignificant interaction between device type and time for each absolute myocardial perfusion outcome. MBF = myocardial blood flow.

edge dissection (n = 2) or lesion length underestimation (n = 1). Procedural non-Q-wave myocardial infarction (maximum creatine kinase MB level 32.4 U · l^{-1}) occurred in 1 patient because of small side branch occlusion after BVS implantation. Non-target vessel revascularization during follow-up was performed in 2 patients in the DES arm, of which 1 was driven by stable angina and 1 was due to non-target vessel myocardial infarction. Five patients (17%) in the DES arm and 4 patients (13%) in the BVS arm

TABLE 3 Positron Emission Tomographic Results Corrected for Resting Rate-Pressure Product

	1 Month	1 Year	3 Years	Interaction (DT × TP)	Main Effects	Delta 1 Month to 1 Year	Delta 1 Month to 3 Years
Corrected resting MBF							
BVS	1.27 ± 0.24	1.21 ± 0.19	1.28 ± 0.24		DT: p = 0.19; TP: p = 0.71	−0.07 ± 0.24	−0.01 ± 0.21
DES	1.16 ± 0.24	1.19 ± 0.32	1.17 ± 0.30	p = 0.38		0.02 ± 0.20	0.02 ± 0.26
All	1.22 ± 0.24	1.20 ± 0.26	1.23 ± 0.27			−0.02 ± 0.22	0.00 ± 0.23
Corrected CPT reserve							
BVS	0.95 ± 0.25	0.89 ± 0.22	0.94 ± 0.26		DT: p = 0.38; TP: p = 0.32	−0.05 ± 0.20	0.01 ± 0.23
DES	0.97 ± 0.29	0.99 ± 0.34	1.04 ± 0.34	p = 0.59		0.01 ± 0.25	0.06 ± 0.31
All	0.96 ± 0.27	0.94 ± 0.29	0.99 ± 0.30			−0.02 ± 0.22	0.03 ± 0.27
Corrected CFR							
BVS	2.44 ± 0.67	2.57 ± 0.95	2.29 ± 0.65		DT: p = 0.03; TP: p = 0.03	0.20 ± 0.89	−0.04 ± 0.67
DES*	2.93 ± 0.63	3.01 ± 1.01	2.70 ± 0.83	p = 0.51		0.08 ± 0.88	−0.30 ± 0.78
All	2.68 ± 0.69	2.79 ± 1.00	2.50 ± 0.76†			0.14 ± 0.87	−0.17 ± 0.73

Values are mean ± SD. Influence of DT and TP on absolute myocardial perfusion was calculated using a mixed-model analysis including two main effects (DT and TP) and a Bonferroni post hoc analysis when appropriate. Note that the delta values of the perfusion indexes display the change in patients who reached 1-year and 3-year follow-up. *p = 0.03 versus BVS measured over all time points together. †p = 0.02 versus 1 year.

Abbreviations as in Tables 1 and 2.

withdrew during follow-up, resulting in 25 (83%) and 26 (87%) patients with complete PET follow-up data in both treatment arms. Of these, 1 (4%) and 3 (12%) patients refused ICA at 3-year follow-up, respectively. At 3-year follow-up, there was 1 significant lesion in the originally treated coronary segment in both treatment arms requiring percutaneous intervention after completion of complete follow-up.

MYOCARDIAL PERFUSION. PET perfusion results for resting MBF, CPT, hyperemic MBF, CPT reserve, and CFR, including the absolute changes from 1 month to 1- and 3-year follow-up, respectively, are presented in Table 2. The primary study endpoint, interaction between device type and time, was nonsignificant for hyperemic MBF, CPT reserve, and CFR (Central Illustration) ($p > 0.05$ for all), meaning that the device type and the time from implantation did not influence each other. Bonferroni post hoc testing revealed that within the total cohort of patients, hyperemic MBF significantly decreased from 1 to 3 years ($p = 0.02$), while CFR was lower at 3-year follow-up compared with 1-month and 1-year follow-up ($p = 0.03$ for both). There was a trend ($p = 0.06$) toward an increase in CPT MBF from 1 to 3 years within the whole patient population. There were no significant differences for resting MBF, CPT MBF, hyperemic MBF, CPT reserve, or CFR between the 2 treatment arms ($p > 0.05$ for all). After correction for resting RPP, corrected CFR was significantly lower for BVS over all time points together compared with DES (Table 3) ($p = 0.03$). Representative invasive coronary angiographic (baseline and 3-year follow-up) and PET perfusion (3-year follow-up) images of a patient with a BVS and a patient with a DES are depicted in Figure 1.

QCA. Table 4 illustrates the quantitative coronary angiographic results of both treatment arms. Mean lesion length was 10.21 ± 4.69 and 10.08 ± 3.82 mm for the BVS and the DES, respectively ($p = 0.91$). MLD was not significantly different between treatment arms prior to intervention ($p = 0.48$). The acute luminal gain due to device implantation was lower within the BVS treatment arm ($p = 0.02$), which resulted in lower MLD and increased %DS post-PCI ($p < 0.01$ and $p < 0.01$, respectively). Differences in MLD and %DS were no longer observed at 3-year follow-up ($p = 0.33$).

OCT. OCT was successfully performed in 29 of 30 patients in both treatment arms at baseline and 24 and 21 patients at 3-year follow-up in the BVS and DES arms, respectively (Tables 5 and 6). Figure 2 shows an example of ICA and OCT for the BVS and the DES prior to PCI, immediately post-PCI, and at 3-year follow-up. Immediately after device implantation and post-dilatation if indicated, MLA and %AS were not significantly different between treatment arms ($p = 0.71$ and $p = 0.78$, respectively). Post-PCI expansion index was significantly lower within the BVS treatment arm, whereas asymmetry index and eccentricity index were comparable between the BVS and DES treatment arms. Percentage malapposed struts was comparable at baseline and 3-year follow-up between the BVS and the DES ($p = 0.08$ and $p = 0.51$, respectively). The percentage of uncovered struts at 3-year follow-up was higher in the DES group ($p < 0.01$). Figure 3 illustrates that there was a

FIGURE 1 **Representative Invasive Coronary Angiographic and Positron Emission Tomographic Perfusion for Bioresorbable Everolimus-Eluting Scaffold and Drug-Eluting Stent**

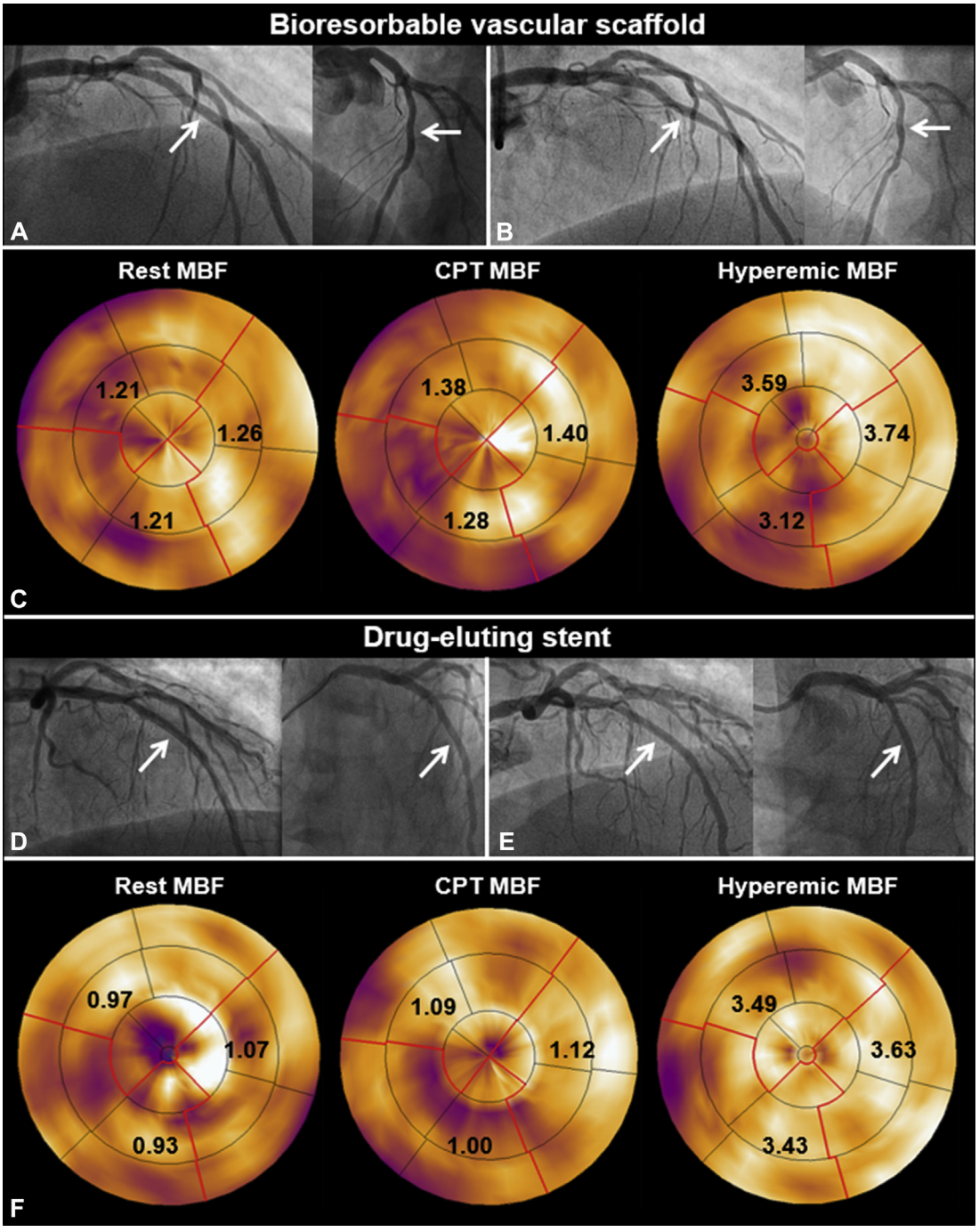

(A) Invasive coronary angiography (ICA) showed a good angiographic result from 2 different angles **(arrows)** immediately after successful bioresorbable everolimus-eluting scaffold (BVS) implantation in the mid left anterior descending coronary artery (LAD). At 3-year follow-up, the scaffold was patent on ICA **(B, arrows)**, and positron emission tomography (PET) **(C)** showed normal rest myocardial blood flow (MBF) that slightly increased during a cold pressor test (CPT), as well as normal MBF during hyperemia. **(D)** ICA demonstrated the immediate result after successful drug-eluting stent implantation in the mid LAD **(arrows)**. At 3-year follow-up, the stent remained patent **(E, arrows)**, and PET **(F)** showed normal MBF during rest with a small increase during a CPT, alongside normal MBF during hyperemia.

TABLE 4 Quantitative Coronary Angiography

	BVS	DES	p Value
Lesion length (mm)	10.21 ± 4.69	10.08 ± 3.82	0.91
Reference vessel diameter (mm)			
Pre-procedure	2.69 ± 0.42	2.66 ± 0.47	0.81
Post-procedure	2.72 ± 0.40	2.83 ± 0.51	0.36
3-yr follow-up	2.66 ± 0.31	2.77 ± 0.45	0.32
Minimal luminal diameter (mm)			
Pre-procedure	0.80 ± 0.29	0.86 ± 0.32	0.48
Post-procedure	2.23 ± 0.35	2.59 ± 0.50	<0.01
3-yr follow-up	2.03 ± 0.38	2.23 ± 0.49	0.13
Acute gain	1.42 ± 0.51	1.73 ± 0.52	0.02
Late loss	0.16 ± 0.38	0.37 ± 0.45	0.10
Net gain	1.25 ± 0.51	1.41 ± 0.48	0.29
Percentage diameter stenosis			
Pre-procedure	68.72 ± 13.62	67.78 ± 9.92	0.76
Post-procedure	18.10 ± 9.75	9.22 ± 7.03	<0.01
3-yr follow-up	23.19 ± 11.92	19.80 ± 11.34	0.33
Binary restenosis at 3-yr follow-up	1 (3.3)	1 (3.3)	1.00

Values are mean ± SD or n (%).
Abbreviations as in Table 1.

significant decrease in MLA and an increase in %AS from baseline (post-PCI) to 3-year follow-up within the BVS arm, whereas no difference over time was observed within the DES arm. In the BVS arm at 3-year follow-up, %AS was significantly higher in comparison with the DES arm ($p = 0.03$), and a trend was observed toward lower MLA ($p = 0.08$).

DISCUSSION

The present study was conducted to assess the evolution of quantitative MBF during endothelium-dependent vasodilation by cold pressor testing and maximal hyperemia by intravenous administration of adenosine after BVS implantation compared with conventional metallic DES over a 3-year period. The main results indicate that there was no significant difference in evolution of CPT reserve, hyperemic MBF, and CFR over time after BVS versus metallic DES implantation. After correction for resting RPP, CFR was significantly lower within the BVS treatment arm. Additionally, QCA illustrated that implantation of BVS resulted in less acute luminal gain, which caused lower MLD and increased %DS immediately post-PCI. Furthermore, optical coherence tomographic analyses revealed a significant decrease in MLA and an increase in %AS from baseline (post-PCI) to 3-year follow-up within the BVS arm, whereas no apparent change was observed within the DES arm. This resulted in a significantly higher %AS with the BVS compared with the DES at 3 years after implantation.

MYOCARDIAL PERFUSION DURING COLD PRESSURE TESTING. Metabolically mediated increase in blood flow after acute cold exposure is an important determinant of coronary vasomotor response to sympathetic activation. Sympathetic activation provokes endothelium-dependent vasodilation of the coronary arteries in case of normal coronary circulation. In the presence of endothelial dysfunction, the metabolically mediated increase of flow is offset by the β-adrenergically stimulated vasoconstriction (14). An impaired response to the CPT is therefore related to vascular dysfunction and the occurrence of adverse cardiac events (6). Previous pioneering preclinical and clinical studies have shown that alongside resorption of the BVS, coronary segments regained the ability to respond to the administration of intracoronary acetylcholine, an endothelium-dependent vasodilator (17,18). More recently, contradicting evidence has become available. The randomized ABSORB II trial found no superiority in vasomotor reaction to pharmacological stimuli for BVS with respect to the metallic stent at 3-year follow-up (19). Dudek et al. (20), who demonstrated that the degree of vasomotor response of the originally stented segment with BVS remained lower in comparison with adjacent segments, further substantiated these findings. However, no studies have been performed using the CPT, which is the gold standard for evaluation of endothelial function by sympathetic stimulation. In the present study, there were no differences observed in responsiveness to CPT between BVS and DES. This may imply that vasomotor function is not largely restored or that minor changes in responsiveness to CPT may be antagonized by diffuse CAD (3). Moreover, responsiveness to sympathetic stimuli is highly affected by age and traditional CAD risk factors (i.e., hypertension, hypercholesterolemia, and smoking), even in the absence of flow-limiting CAD (21). Although falling short in statistical significance, there were numerically more current smokers in the BVS group, which may have neutralized the postulated favoring effect of scaffold resorption on vasomotor function (21). Consequently, we cannot genuinely conclude that there is no recovery of epicardial vasomotor function on the basis of the results of the present study, but any substantial magnitude on myocardial perfusion after cold pressor testing was not observed.

IMPACT OF BVS RESORPTION ON HYPEREMIC MYOCARDIAL PERFUSION AND CFR. It has been shown that even in the absence of a coronary lesion, a reduction in MBF is associated with the occurrence of major adverse cardiac events (4,5). Data regarding the

TABLE 5 Optical Coherence Tomography After Percutaneous Coronary Intervention and at 3-Year Follow-Up

	n	BVS	n	DES	p Value
Reference luminal area (mm^2)					
Post-PCI	29	7.89 ± 1.82	29	8.20 ± 2.30	0.58
3-yr follow-up	24	7.51 ± 1.80	21	7.97 ± 2.84	0.52
Minimal luminal area (mm^2)					
Post-PCI	29	5.84 ± 1.49	29	6.01 ± 1.94	0.71
3-yr follow-up	24	4.27 ± 1.59	21	5.33 ± 2.35	0.08
Percentage area stenosis (%)					
Post-PCI	29	24.90 ± 13.55	29	25.93 ± 14.38	0.78
3-yr follow-up	24	44.05 ± 14.83	21	33.45 ± 16.90	0.03
Percentage malapposed struts (%)					
Post-PCI	29	0.00 (0.00 to 1.50)	29	0.85 (0.00 to 3.37)	0.08
3-year follow-up	24	0.00 (0.00 to 0.00)	21	0.00 (0.00 to 0.00)	0.51
Minimal endoluminal scaffold/stent area (mm^2)					
Post-PCI	29	5.39 ± 1.58	29	6.27 ± 1.99	0.07
3-yr follow-up	24	5.20 ± 2.22	21	6.74 ± 2.13	0.02
Scaffold/stent-based percentage area stenosis (%)					
Post-PCI	29	31.26 ± 13.21	29	22.96 ± 14.14	0.02
3-yr follow-up	24	26.05 (13.53 to 37.54)	21	12.28 (−1.85 to 27.55)	<0.01
Post-PCI implantation results					
Asymmetry index	29	0.38 ± 0.08	29	0.38 ± 0.08	0.90
Asymmetric lesion	29	25 (86)	29	24 (83)	1.00
Eccentricity index	29	0.72 ± 0.08	29	0.72 ± 0.06	0.88
Eccentric lesion	29	10 (34)	29	11 (38)	1.00
Expansion index (%)	29	68.74 ± 13.21	29	77.04 ± 14.14	0.02
Optimal stent/scaffold expansion	29	9 (31)	29	12 (41)	0.59
3-year follow-up					
Mean neointimal area (mm^2)	24	1.32 ± 0.46	21	1.14 ± 0.48	0.23
Maximum neointimal area (mm^2)	24	2.15 ± 0.73	21	2.43 ± 1.28	0.39
Percentage uncovered struts	24	0.00 (0.00 to 0.00)	21	0.00 (0.00 to 1.02)	<0.01
Neointimal strut coverage (mm)	24	0.16 ± 0.04	21	0.13 ± 0.06	0.12

Values are mean ± SD, median (interquartile range), or n (%). Presented data are unpaired because of differences in number of patients at post-PCI and 3-year follow-up. The changes between post-PCI and 3-year follow-up measurements presented in this table should therefore be interpreted with caution and may be induced by differences in included patients at timing of evaluations.

PCI = percutaneous coronary intervention; other abbreviations as in Table 1.

effect of scaffold resorption on absolute MBF in patients in stable condition is lacking. The present study showed that there was no significant interaction between device type and follow-up time for resting and hyperemic MBF or CFR. These findings denote that resorption of BVS did not alter the vessels' ability to increase hyperemic MBF or CFR compared with metallic DES up to 3 years after implantation. Notwithstanding, comparable efficacy of BVS and DES in terms of absolute perfusion during hyperemia in patients with stable CAD was observed. These findings are in line with the ABSORB TROFI II trial, a randomized clinical trial of BVS versus metallic DES for treatment of infarct-related lesions, demonstrating adequate and similar invasively measured functional microcirculatory parameters between both treatment arms at 3-year follow-up. Moreover, absolute flow by intracoronary thermodilution was similar between treatment arms (22). Myocardial perfusion is the composite effect of focal, diffuse, and microvascular disease (23). Hypothetically, restoration of epicardial vessel physiology due to scaffold resorption may not translate into an apparent increase in perfusion on the myocardial level, because of a transcending and counterweighting effect of diffuse and microvascular disease in patients with established CAD. Results for hyperemic MBF and CFR were similar in the myocardial areas of nontreated vessels in the same patient (data not shown), supporting the

TABLE 6 Optical Coherence Tomography Not Performed or Insufficient Quality

	BVS	DES
Post-PCI		
Insufficient contrast delivery	1 (3.3)	1 (3.3)
3-yr follow-up		
Insufficient contrast delivery	1 (3.3)	1 (3.3)
Withdrew from study	4 (13.3)	5 (16.7)
Refused ICA	1 (3.3)	3 (10.0)

Values are n (%).

ICA = invasive coronary angiography; other abbreviations as in Tables 1 and 5.

FIGURE 2 Representative Invasive Coronary Angiographic and Optical Coherence Tomographic Images Before, Immediately After, and at 3-Year Follow-Up After Bioresorbable Everolimus-Eluting Scaffold and Drug-Eluting Stent Implantation

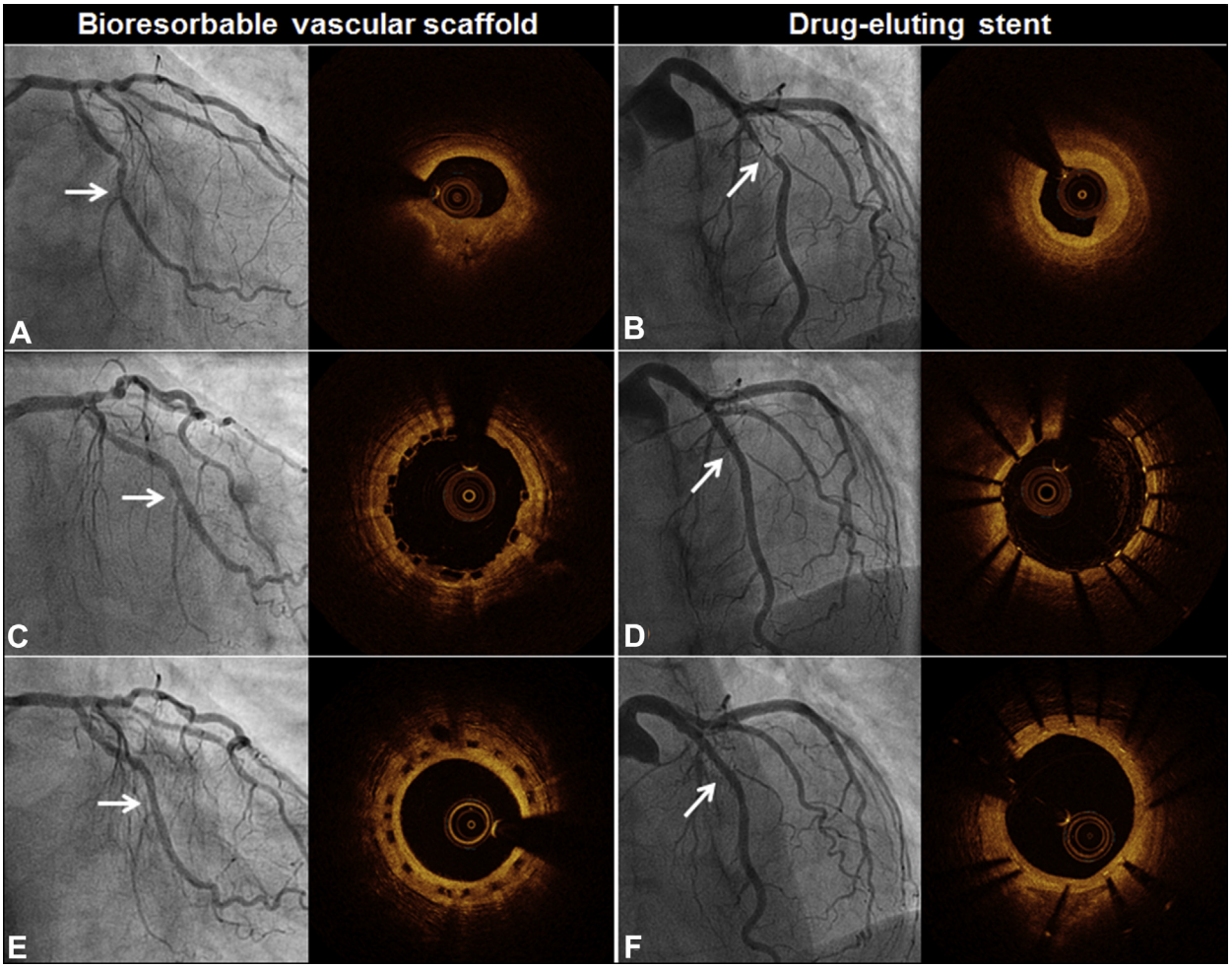

A severe stenosis **(arrow)** in the mid left circumflex coronary artery **(A)** and a severe stenosis **(arrow)** in the proximal left anterior descending coronary artery **(B)**, with optical coherence tomography (OCT) showing the most affected sides. Both lesions were successfully treated with a bioresorbable everolimus-eluting scaffold (BVS) **(C, arrow)** and a drug-eluting stent (DES) **(D, arrow)**, as is shown with invasive coronary angiography (ICA) and OCT immediately after implantation. At 3-year follow-up after BVS implantation **(E)** and DES implantation **(F)**, ICA showed a good angiographic result with a patent device **(arrows)**, while OCT showed a small layer of neointimal tissue and limited loss of lumen area within the device.

limited effects of vessel "caging" on hyperemic myocardial perfusion and CFR. In addition, decreases in hyperemic MBF and CFR were observed within the complete study population together at 3-year follow-up, which may further support the effect of atherosclerotic progression on myocardial perfusion in patients with CAD.

QCA AND OCT. Acute luminal gain due to device implantation, as measured with QCA, was lower within the BVS treatment arm, which resulted in lower MLD and increased %DS post-PCI. This difference in MLD and %DS was not observed at 3-year follow-up. Sotomi et al. (24) previously showed that in-device luminal dimension measurements after BVS implantation are underestimated using QCA, probably because of polymer strut protrusion in the coronary lumen, and this could have induced an unfavorable difference in MLD and acute luminal gain post-PCI for BVS (24). Moreover, after 3-year follow-up, OCT analyses showed higher %AS and a trend toward lower MLA with the BVS compared with the DES. These results were consistent when using scaffold or stent area as a reference

to calculate area stenosis, an analysis that was performed to limit bias potentially introduced by reference vessel diameter. In line with the present study results, the randomized China ABSORB trial observed that within device post-PCI MLD and acute gain were lower with BVS compared with metallic DES, and %DS was slightly greater (25). In addition, the ABSORB II trial observed a difference in MLA by intravascular ultrasound assessment at 3-year follow-up (BVS vs. DES: 4.32 ± 1.48 mm^2 vs. 5.38 ± 1.51 mm^2; $p < 0.0001$) (19). These results are essentially similar to the optical coherence tomographic observations at 3-year follow-up in the present study (BVS vs. DES: 4.27 ± 1.59 mm^2 vs. 5.33 ± 2.35 mm^2; p=0.08). Interestingly, this difference did not evidently translate into lower myocardial perfusion during CPT and hyperemia. Yet after correction for resting RPP (i.e. cardiac work load), CFR was significantly lower for BVS when comparing over all time points together, which may be explained by an increase in %AS. There were 2 patients (1 with a DES and 1 with a BVS) with significant restenoses in the originally stented segments, and in 1 patient (with a DES), a significant stenosis was observed distally from the stented segment at 3-year follow-up. A clear perfusion decrease between 1 month and 3 years was observed in only in 1 of these 3 patients within the DES arm. During inclusion for the present study, the instructions for BVS implantation developed, and accurate pre-dilation, scaffold sizing, and post-dilation have been strongly advised to minimize scaffold-related hard events. Although this technique was not performed systematically within the present study, all stent and scaffold implantations were OCT guided, which is documented to optimize PCI outcomes acutely and in the long term (26). Stent and scaffold sizing was based on dimensions measured by OCT, and additional post-dilation was performed in case of suboptimal scaffold or stent deployment. Rates of optimal stent and scaffold deployment were not significantly different between the groups (**Table 5**).

FIGURE 3 Baseline and Follow-up Optical Coherence Tomography

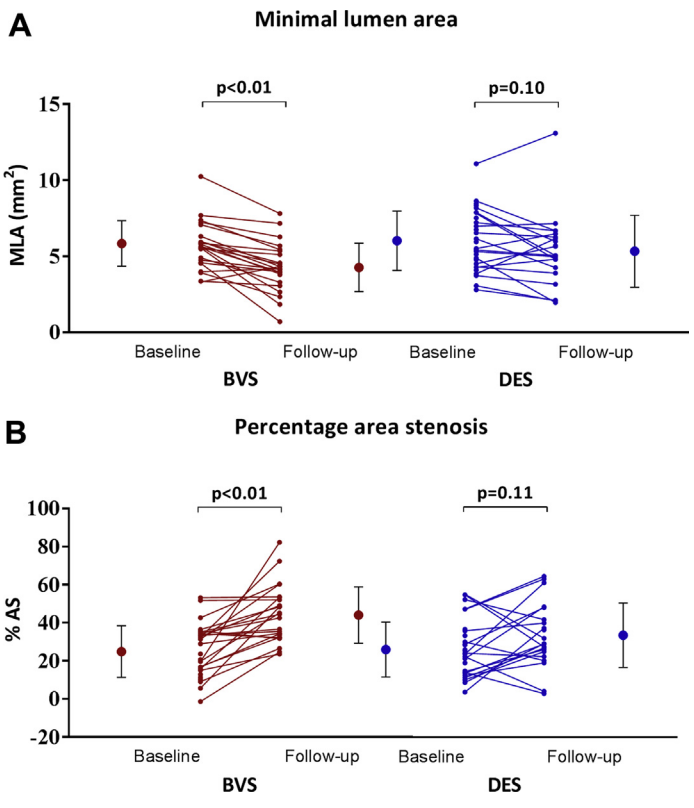

Changes in minimal luminal area (MLA) **(A)** and percentage area stenosis (%AS) **(B)** over time, measured by optical coherence tomography at baseline (post-percutaneous coronary intervention) and 3-year follow-up are shown for the bioresorbable everolimus-eluting scaffold (BVS) and drug-eluting stent (DES) treatment arms, respectively. The **circle** and **error bars** represent the mean and SD and are given for the measurements at baseline and at follow-up in both the BVS and DES treatment arms.

STUDY LIMITATIONS. Although blinded randomization was performed, the BVS group included numerically more left circumflex coronary arteries. These incidental differences in targeted coronary arteries between treatment arms may have affected the results. Moreover, the downstream extent of myocardial area is generally smaller for the left circumflex coronary artery, which may have interfered with the potential benefit of BVS implantation. Furthermore, the BVS group involved nonsignificant but numerically more patients with unstable angina compared with the DES treatment arm. Because the extent of atherosclerotic inflammation, as seen in patients with unstable plaques, may decrease the ability of coronary vessels to respond to cold pressor testing and pharmacological stimuli, beneficial effects of scaffold resorption could have been diminished within the BVS population.

The sample size was calculated to detect differences in mean changes in outcomes between devices using 0.8 times the SD of the outcome. This cutoff was chosen on the basis of the interscan difference, but smaller differences between both treatment arms may not have been found significant, because of the wide confidence interval and relatively small sample size.

Perfusion imaging prior to inclusion was not performed by design of the study. Therefore, differences

in recovery of myocardial perfusion due to implantation of BVS versus metallic DES were not assessed. Implantation of both BVS and DES reinstates vessel patency, but it could be hypothesized that the larger strut dimensions of BVS compromise side branch patency.

Although patients were instructed to continue statin therapy according to current international guidelines, adherence to statin therapy during follow-up visits was not documented and could have induced differences in atherosclerotic progression between treatment arms.

Optical coherence tomographic and quantitative coronary angiographic data should be considered hypothesize generating only, because the study was not sufficiently powered to investigate differences in disease progression.

CONCLUSIONS

Up to 3 years, implantation of the BVS did not result in a favorable evolution of hyperemic MBF, CFR, or CPT reserve compared with metallic DES implantation in patients with de novo single-vessel CAD. Angiographic characteristics after BVS implantation seem to be slightly inferior compared with metallic DES.

ADDRESS FOR CORRESPONDENCE: Dr. Paul Knaapen, Department of Cardiology, Amsterdam UMC, VU University Medical Center, De Boelelaan 1117, 1081 HV Amsterdam, the Netherlands. E-mail: p.knaapen@vumc.nl.

PERSPECTIVES

WHAT IS KNOWN? Long-term resorption of the BVS restores normal vessel geometry, allowing natural regeneration of the endothelium.

WHAT IS NEW? The randomized clinical VANISH trial showed that restoration of normal vessel geometry did not translate into improved absolute MBF during 3-year follow-up.

WHAT IS NEXT? These results do not support the use of BVS over DES until benefit with regard to long-term major adverse cardiac events has been shown.

REFERENCES

1. Gogas BD, Farooq V, Onuma Y, Serruys PW. The ABSORB bioresorbable vascular scaffold: an evolution or revolution in interventional cardiology? Hellenic J Cardiol 2012;53:301–9.

2. Serruys PW, Garcia-Garcia HM, Onuma Y. From metallic cages to transient bioresorbable scaffolds: change in paradigm of coronary revascularization in the upcoming decade? Eur Heart J 2012;33:16–25b.

3. Brugaletta S, Heo JH, Garcia-Garcia HM, et al. Endothelial-dependent vasomotion in a coronary segment treated by ABSORB everolimus-eluting bioresorbable vascular scaffold system is related to plaque composition at the time of bioresorption of the polymer: indirect finding of vascular reparative therapy? Eur Heart J 2012;33:1325–33.

4. Taqueti VR, Hachamovitch R, Murthy VL, et al. Global coronary flow reserve is associated with adverse cardiovascular events independently of luminal angiographic severity and modifies the effect of early revascularization. Circulation 2015; 131:19–27.

5. Murthy VL, Naya M, Foster CR, et al. Improved cardiac risk assessment with noninvasive measures of coronary flow reserve. Circulation 2011;124: 2215–24.

6. Kiviniemi T. Assessment of coronary blood flow and the reactivity of the microcirculation non-invasively with transthoracic echocardiography. Clin Physiol Funct Imaging 2008;28: 145–55.

7. Stuijfzand WJ, Raijmakers PG, Driessen RS, et al. Evaluation of myocardial blood flow and coronary flow reserve after implantation of a bioresorbable vascular scaffold versus metal drug-eluting stent: an interim one-month analysis of the VANISH trial. EuroIntervention 2016;12:e584–94.

8. Tearney GJ, Regar E, Akasaka T, et al. Consensus standards for acquisition, measurement, and reporting of intravascular optical coherence tomography studies: a report from the International Working Group for Intravascular Optical Coherence Tomography Standardization and Validation. J Am Coll Cardiol 2012;59: 1058–72.

9. Nakatani S, Sotomi Y, Ishibashi Y, et al. Comparative analysis method of permanent metallic stents (XIENCE) and bioresorbable poly-L-lactic (PLLA) scaffolds (Absorb) on optical coherence tomography at baseline and follow-up. EuroIntervention 2016;12:1498–509.

10. Suwannasom P, Sotomi Y, Ishibashi Y, et al. The impact of post-procedural asymmetry, expansion, and eccentricity of bioresorbable everolimus-eluting scaffold and metallic everolimus-eluting stent on clinical outcomes in the ABSORB II trial. J Am Coll Cardiol Intv 2016;9:1231–42.

11. Onuma Y, Serruys PW, Perkins LE, et al. Intracoronary optical coherence tomography and histology at 1 month and 2, 3, and 4 years after implantation of everolimus-eluting bioresorbable vascular scaffolds in a porcine coronary artery model: an attempt to decipher the human optical coherence tomography images in the ABSORB trial. Circulation 2010;122:2288–300.

12. Andreasen LN, Holm NR, Balleby IR, et al. Randomized comparison of sirolimus eluting, and biolimus eluting bioresorbable polymer stents: the SORT-OUT VII optical coherence tomography study. Eur Heart J Cardiovasc Imaging 2018;19: 329–38.

13. Danad I, Raijmakers PG, Appelman YE, et al. Coronary risk factors and myocardial blood flow in patients evaluated for coronary artery disease: a quantitative $[^{15}O]H_2O$ PET/CT study. Eur J Nucl Med Mol Imaging 2012;39:102–12.

14. Schindler TH, Nitzsche EU, Olschewski M, et al. PET-measured responses of MBF to cold pressor testing correlate with indices of coronary vasomotion on quantitative coronary angiography. J Nucl Med 2004;45:419–28.

15. Harms HJ, Knaapen P, de Haan S, Halbmeijer R, Lammertsma AA, Lubberink M. Automatic generation of absolute myocardial blood flow images using $[^{15}O]H_2O$ and a clinical PET/CT scanner. Eur J Nucl Med 2011;38:930–9.

16. Cerqueira MD, Weissman NJ, Dilsizian V, et al. Standardized myocardial segmentation and nomenclature for tomographic imaging of the heart. A statement for healthcare professionals from the Cardiac Imaging Committee of the Council on Clinical Cardiology of the American Heart Association. Circulation 2002; 105:539–42.

17. Serruys PW, Ormiston JA, Onuma Y, et al. A bioabsorbable everolimus-eluting coronary stent system (ABSORB):2-year outcomes and results from multiple imaging methods. Lancet 2009;373:897–910.

18. Gogas BD, Benham JJ, Hsu S, Sheehy A, Lefer DJ, Goodchild TT, et al. Vasomotor function comparative assessment at 1 and 2 years following implantation of the Absorb everolimus-eluting bioresorbable vascular scaffold and the Xience V everolimus-eluting metallic stent in porcine coronary arteries: insights from in vivo angiography, ex vivo assessment, and gene analysis at the stented/scaffolded segments and the proximal and distal edges. J Am Coll Cardiol Intv 2016;9:728–41.

19. Serruys PW, Chevalier B, Sotomi Y, et al. Comparison of an everolimus-eluting bioresorbable scaffold with an everolimus-eluting metallic stent for the treatment of coronary artery stenosis (ABSORB II): a 3 year, randomised, controlled, single-blind, multicentre clinical trial. Lancet 2016;388:2479–91.

20. Dudek D, Rzeszutko L, Onuma Y, et al. Vasomotor response to nitroglycerine over 5 years follow-up after everolimus-eluting bioresorbable scaffold implantation. J Am Coll Cardiol Intv 2017;10:786–95.

21. Siegrist PT, Gaemperli O, Koepfli P, et al. Repeatability of cold pressor test-induced flow increase assessed with H(2)(15)O and PET. J Nucl Med 2006;47:1420–6.

22. Gomez-Lara J, Brugaletta S, Ortega-Paz L, et al. Long-term coronary functional assessment of the infarct-related artery treated with everolimus-eluting bioresorbable scaffolds or everolimus-eluting metallic stents: insights of the TROFI II trial. J Am Coll Cardiol Intv 2018;11:1559–71.

23. Johnson NP, Kirkeeide RL, Gould KL. Is discordance of coronary flow reserve and fractional flow reserve due to methodology or clinically relevant coronary pathophysiology? J Am Coll Cardiol Img 2012;5:193–202.

24. Sotomi Y, Onuma Y, Suwannasom P, et al. Is quantitative coronary angiography reliable in assessing the lumen gain after treatment with the everolimus-eluting bioresorbable polylactide scaffold? EuroIntervention 2016;12:e998–1008.

25. Gao R, Yang Y, Han Y, et al. Bioresorbable vascular scaffolds versus metallic stents in patients with coronary artery disease: ABSORB China trial. J Am Coll Cardiol 2015;66:2298–309.

26. Jones DA, Rathod KS, Koganti S, et al. Angiography alone versus angiography plus optical coherence tomography to guide percutaneous coronary intervention: outcomes from the Pan-London PCI Cohort. J Am Coll Cardiol Intv 2018;11:1313–21.

KEY WORDS bioresorbable vascular scaffold, myocardial perfusion, percutaneous coronary intervention, position emission tomography